Rapid, modular secondary sphere assembly for enhanced Fe-catalyzed C(sp³)–H oxidation

Sabari Ghosh[†], Phuong Nguyen Tran[†], Dan McElheny[†], Juan J. Perez[†], Andy I. Nguyen[†]*

[†]Department of Chemistry, University of Illinois at Chicago, Chicago, Illinois 60607, United States

ABSTRACT: The inert nature of C(sp³)–H bonds makes their oxidative cleavage a difficult task. While metalloenzymes employ an array of non-covalent interactions to facilitate C(sp³)–H oxidation, this strategy is underexplored in abiotic catalysts due to time-consuming and low-yielding ligand syntheses, which impedes iterative design. To surmount these obstacles, we, herein, have developed a highly modular and rapid synthetic strategy that capitalizes on the efficiency of solid-phase peptide synthesis, which enables the generation of a ligand platform displaying at least four unique residues of varying electronics and sterics in the secondary coordination sphere of a C–H oxidizing Fe catalyst. Modulating the non-covalent interactions in seven variants significantly influences cyclohexane oxidation catalysis, with one variant that boosts the catalytic activity by more than two-fold. To better understand the catalytic trends, we have determined the catalysts' solution-state structures by 2D NMR spectroscopy, which suggests that peptide conformation can control substrate access and binding. This work demonstrates that (1) tunable, diverse, and complex active sites can be made readily, and (2) these active sites can be optimized to significantly increase catalytic activity.

The recalcitrant nature of the C(sp³)–H bond presents a major obstacle for converting abundant hydrocarbon resources into value-added products and opening novel routes for organic synthesis.[1–3] An important example concerns the wasteful flaring of methane during oil production, which could be eliminated by oxidation into methanol, a useful chemical and easily-transportable liquid fuel.[4,5] Though there are a handful of synthetic catalysts that can oxidize C(sp³)–H bonds to alcohol or carbonyl groups, current systems still demonstrate low activity, in contrast to efficient C–H oxidizing metalloenzymes – such as soluble methane monooxygenase (sMMO), particulate methane monooxygenase (pMMO), and cytochrome P450 (Figure 1A)[10,11].[6–9] Abiotic catalysts are more advantageous compared to enzymes in that their function and structure are not limited to what is biologically available, but the architecture of current catalysts have few options to engineer a secondary coordination sphere that could assist in substrate binding or reactive species generation.[6] Some notable examples of catalysts have explored the use of non-covalent interactions in the secondary sphere to improve C–H oxidation (Figure 1B), but the drawbacks of these aforementioned catalysts are their lengthy syntheses and low modularity, which limits designability and optimization.[12–19]

We hypothesize that synthetic peptides, which possess enormous structural diversity and are quickly assembled with robust, low-cost, and high-yielding chemistry, would overcome previous synthetic bottlenecks associated with secondary sphere synthesis.[20–23] While many laboratories have explored peptides to tune the primary coordination sphere[24–30], fewer have targeted the secondary sphere,[31–37] and to our knowledge, there are no metallopeptides that utilize the secondary sphere to optimize C(sp³)–H oxidation. Herein, we report a modular peptidic platform that display four unique residues in secondary sphere and can enhance the activity of a Fe-based C(sp³)–H oxidation catalyst.

Our catalyst design (Figure 1C) incorporates the following: (1) precise covalent attachment of a known catalytic inorganic complex, (2) a well-structured macromolecular peptide positioned above the cofactor to display various functionalities, and (3) a minimalist design to facilitate understanding of structure-function relationships. We targeted the Fe complexes of *tris*-(2-pyridylmethyl)amine (TPA) first described by Que and coworkers,[6] which catalyze the oxidation of cyclohexane to cyclohexanol and cyclohexanone using the atom economical oxidant H_2O_2 via a well-established mechanism.[38] Recent reports have shown that TPA and similar ligands can be covalently attached to the N-terminus of a helical peptide such that the metal center is proximal to several sidechains.[39,40] Based on this previous work, we postulated that a metal-containing active site pocket can be readily constructed by dimerization of the peptide scaffolds, such as by disulfide bond formation via an incorporated cysteine residue.[41]

Our general sequence design comprises mostly the non-canonical amino acid 2-aminoisobutyric acid (Aib, one letter code = B), which reliably folds peptides into a 3_{10}-helical secondary structure (Table 1).[20,21,23] In this sequence, a 3_{10} helix places residue 7 distal from, but positioned directly above the TPA cofactor, and thus was chosen to be cysteine to allow for dimerization via disulfide bond formation.[42] Residues 3 and 4 are in close proximity to the TPA cofactor, and combinations of glutamine and alanine in those positions were synthesized to probe the effects of hydrogen bonding and sterics around the metal. Peptides were synthesized by solid-phase peptide synthesis (SPPS),[43] and importantly, purified peptide can be obtained with straightforward protocols in ~3 days with high yields. All peptides in this report fold well into a 3_{10} helix (in 1:9 H_2O:MeCN) as exhibited by similar features in circular dichroism (CD) spectrum: a negative band at ~208 nm with a broad shoulder at ~222 nm and some positive intensity at 195 nm (Figure S8).[44,45]

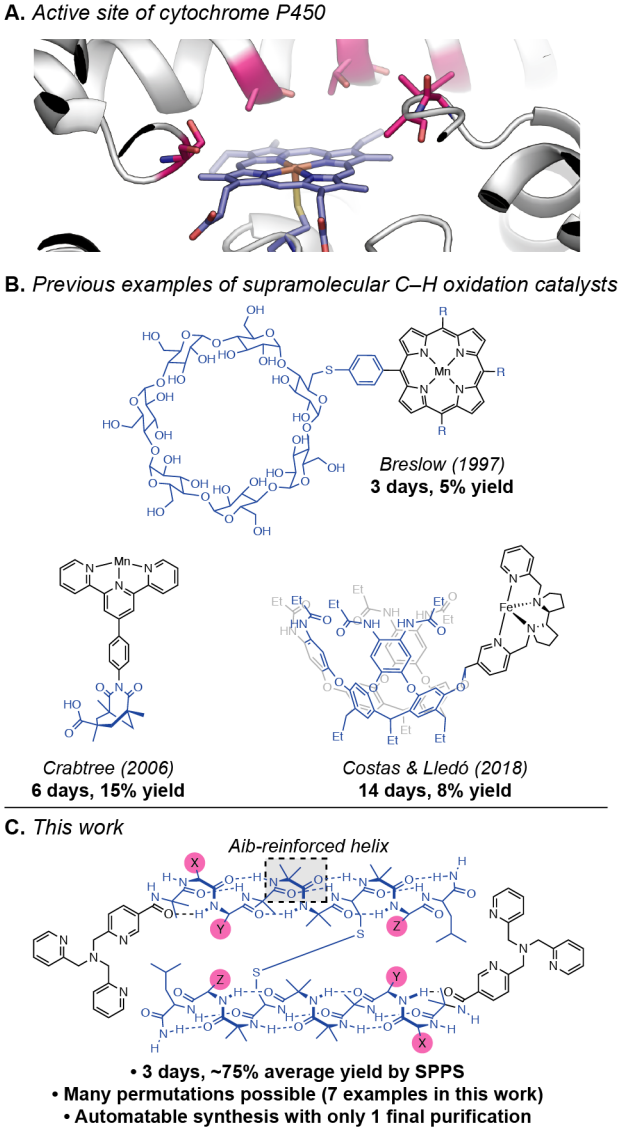

Figure 1. (A) Active site of cytochrome P450 highlighting the secondary sphere colored in magenta. (B) Representative selection of C–H oxidation catalysts that use a supramolecular secondary sphere. Their synthesis times (excluding those of purification steps) and yields of only the supramolecular units are shown.[46–50] (C) This work uses dimeric peptide helices to construct the secondary sphere.

Table 1. Peptide sequences in this report

Name	Sequence [a]
A3Q4	TPA-B**AQ**BBCBL-NH2
Q3Q4	TPA-B**QQ**BBCBL-NH2
A3A4	TPA-B**AA**BBCBL-NH2
Q3A4	TPA-B**QA**BBCBL-NH2
A3A4F8	TPA-B**AA**BBC**F**L-NH2
A3E4	TPA-B**AE**BBCBL-NH2
A3A4-OH	TPA-B**AA**BBCBL-**OH**

[a] The peptides are homodimers, but only the sequence of one chain is shown

Metalation with $Fe(OTf)_2$ afforded bright yellow complexes consistent with previously reported $Fe(TPA)^{+2}$ complexes (SI).[6] CD spectra confirmed that the helical structures were maintained after metalation. The NMR spectra of the Fe^{II} complexes exhibited very broad resonances indicating a significant population of paramagnetic, high-spin Fe^{II}, preventing structural determination by NMR spectroscopy.[38] In order to obtain representative NMR structures, 2D spectra were collected on diamagnetic Zn^{II} analogs (Figure 2). The ^1H NMR spectra of all Zn^{II} complexes show only one set of peaks indicating symmetrically-related helices, and a pattern of NOE cross peaks defining a 3_{10} helix (SI).[51] In **Q3Q4** and **A3Q4**, the ε-NH_2 protons of Q4 are noticeably broader (FWHM of 35 Hz and 56 Hz, respectively) than other amide protons suggesting faster exchange with H_2O, consistent with binding of the amide carbonyl oxygen to the Lewis acidic Zn^{II} center.[52] More importantly, there are several NOE cross peaks between residues distant in the sequence that are not possible within a single chain, revealing that the helices are antiparallel with respect to each other. The NMR-derived distance constraints were used to solve the structures of Zn-peptides. Complexes of **X3Q4** (X = A or Q) show coordination of Q4 to the metal allowing the ε-NH_2 group to act as a secondary sphere H-bond donor, while the opposing helix is pushed away by the sterics of Q4. Moreover, in **Q3Q4**, H-bonding between Q3 and L9's carboxamide pulls the helix further way from TPA than in **A3Q4**. Mutation of **X3Q4** to **X3A4** (X = A or Q) allows the opposing helix to swing closer to TPA, with the identity of residue 3 controlling the level of helical movement. In **Q3A4,** a H-bond between L9 to Q3 allows the two helices to create a hydrophobic cavity above the metal center lined with Ala or Aib residues. In **A3A4**, the absence of interchain H-bonding coupled with small size of residue A4, allows the C-terminus to approach even closer to the metal center, ~4 Å between the carboxamide and the metal center. Thus, the side chains control precise placement of functional groups in the secondary sphere of the TPA site.

Indeed, the catalytic oxidation of cyclohexane by H_2O_2 (in MeCN) mediated by the Fe-peptide complexes clearly reveals the effect of secondary coordination sphere when compared to the cofactor analog, $Fe(5\text{-}MeO_2C\text{-}TPA)(OTf)_2$ (Figure 3). The overall oxidation yield by **Fe_2(Q3Q4)** is 27% higher than that of the pure cofactor, $Fe(5\text{-}MeO_2C\text{-}TPA)$, with increased cyclohexanone production accounting for higher yield. Mutation to **Fe_2(A3Q4)** greatly increases the turnover of the catalyst (82% higher than cofactor), which is surprising since there is only a subtle variation between the helix orientation compared to **Fe_2(Q3Q4)** (*vide supra*). This observation showcases that catalysis is highly sensitive to even minor changes in the secondary coordination sphere. The catalytic activity is further improved upon mutation to **Fe_2(X3A4)** (X = A or Q). The slight differences at the helical interface between Q3A4 and A3A4 (*vide supra*) manifests in small, but significant differences in activity (116% and 103% higher than cofactor for Q3A4 and A3A4, respectively). The Q4A mutation removes the coordination of Q4 from the metal center, but it is important to note that the elevated activity is not solely attributable to the increase in metal coordination sites since these mutants exhibit similar primary coordination as $Fe(5\text{-}MeO_2C\text{-}TPA)$.[6] These observations suggest that the peptidic secondary sphere plays an essential role, either by enhancing the formation of catalyst-substrate complex or disfavoring the nonproductive disproportionation of H_2O_2. The higher proportion of ketone

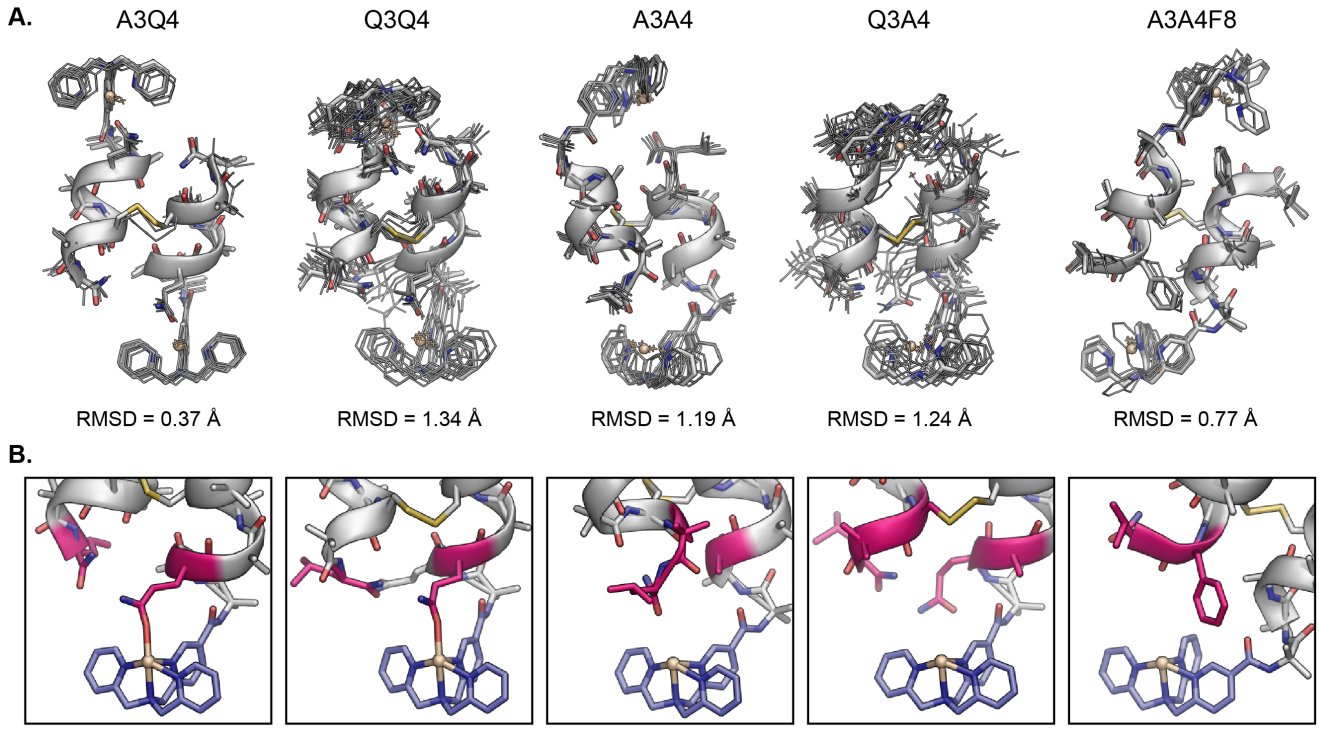

Figure 2. (A) NMR solution structures of Zn^{+2} metallated peptides in 1:9 H_2O:CD_3CN. Ensembles of the ten lowest-energy structures are shown, with the most stable structure shown in ribbon and stick representation. Zinc atoms are represented by yellow spheres. (B) Close-up of the active site in the lowest-energy structure. The relevant residues in the secondary sphere are highlighted in magenta.

produced by all peptide catalysts in comparison to Fe(5-MeO_2C-TPA) may also be explained by a stronger retention of cyclohexanol by the peptide scaffold, favoring a second oxidation event.

Mutations of residues far from TPA in the sequence can also appreciably influence catalysis through the geometry imparted by the antiparallel helices. The B8F mutation in **A3A4** (**A3A4F8**) drastically reduces the catalytic activity (12% *less* than the cofactor). Examination of the NMR structure of **A3A4F8** provides a likely explanation, which is that the position of F8 over the TPA cofactor may obstruct substrate access.

Addition of excess acetic acid has been known to greatly increase the yield of C–H oxidation by Fe catalysts, and this effect has been hypothesized to operate via an Fe^{III}–HOAc intermediate that facilitates conversion of Fe^{III}–OOH to the active Fe^{V}=O species.[53–56] This mechanistic proposal inspired us to mutate Q4 to an isostructural glutamic acid and examine its effect on cyclohexane oxidation. **Fe_2(A3E4)** has very similar spectroscopic features to **Fe_2(A3Q4)** (NOESY features in Zn analogs are also comparable), suggesting an analogous structure; however, the catalytic activity is mostly unchanged, demonstrating that the Fe-bound carboxylic acid does not play a major role in catalysis, at least in this coordination mode. As noted in previous studies, the exact role of acetic acid in Fe-catalyzed C–H oxidation remains ambiguous,[53,54] and our findings suggest that simple coordination of a carboxylic acid may not be enough to increase activity. We further tested another site for introducing a carboxylic acid at the C-terminus of **A3A4**, which is in close proximity to the cofactor due to the antiparallel orientation of the helices. This mutant, **Fe_2(A3A4-OH)**, however, shows much less activity than **Fe_2(A3A4),** which further illustrates that the function of carboxylic acids may be more complicated than in what has been previously proposed.[54,56]

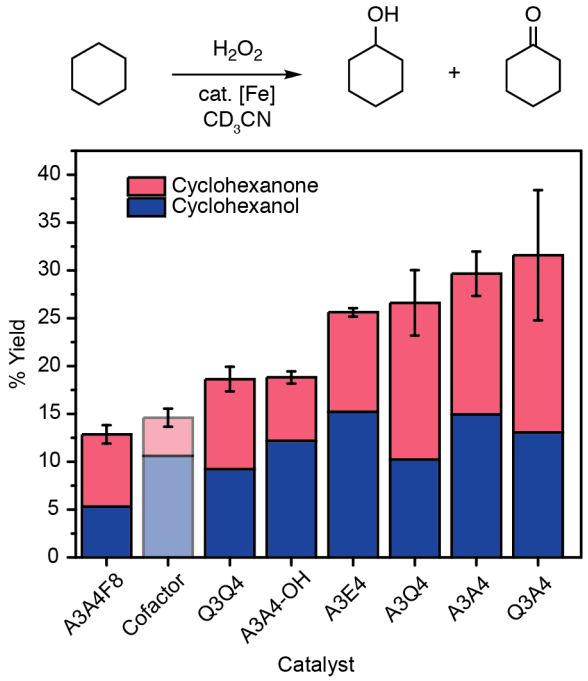

Figure 3. Catalytic oxidation of cyclohexane by iron complexes (Fe:H_2O_2:cyclohexane is 1:10:100). Yields are averaged from three runs and calculated with respect to the limiting reagent, H_2O_2. Error bars correspond to the total yield. Cofactor is Fe(5-MeO_2C-TPA)$(OTf)_2$.

Due to the abundance of C–H bonds in the scaffold, we investigated the fate of the peptides after catalysis. Liquid chromatography–mass spectrometry of the post-catalytic solutions revealed major species consistent with disulfide bond cleavage and addition of three oxygen atoms (Figure S61-S67). To locate the oxygenated residue(s), the peptides were sequenced by MS/MS, and surprisingly, while no C–H bonds were identified to be hydroxylated, C7 was completely oxidized to cysteic acid in all cases (Figure S61-S67). Usually, oxidation of disulfides to cysteic acid requires harsh conditions, such as concentrated performic acid.[57] Cysteic acid formation likely deactivates catalysis by neutralizing the catalytically relevant Fe^{III}–OH moiety,[54] as evidenced by the fact that additional equivalents of H_2O_2 do not further increase yield of cyclohexane oxidation (Table S22). This observation pinpoints the disulfide motif as a weak link and will guide the evolution of future design towards other peptide dimerization techniques.[58–60]

The strategy presented in this work – the combination of non-canonical residues to control secondary structure, dimerization of helices to generate active site, and conjugation of a catalytic unit – provides a practical and versatile route for secondary sphere ligand design. The ability of this ligand platform to improve upon the highly challenging catalytic oxidation of $C(sp^3)$–H bonds attests to the influential role of non-covalent interactions in the active site microenvironment. We anticipate that the modularity and expandability of the scaffold will enable nearly endless permutations for engineering this microenvironment for regio- and stereoselectivity. Though the structure-space of peptides is vast, the ease and speed of making these ligands is expected to allow for high-throughput synthesis and directed evolution approaches to uncover highly active variants. Lastly, the synthetic and design approach in this work should be widely adaptable to a number of other catalysis.

ASSOCIATED CONTENT

Supporting Information

Synthesis and characterization details (NMR spectroscopy, mass spectrometry, LC-MS, CD spectroscopy, UV-vis spectroscopy) are provided in the Supporting Information.

The Supporting Information is available free of charge on the ACS Publications website.

AUTHOR INFORMATION

Corresponding Author

* andyn@uic.edu

Author Contributions

A.I.N. and S.G. formulated the project. S.G., P.N.T., and J.J.P carried out the experiments. D.M. developed the workflow for solving the NMR structures.

Funding Sources

This research was supported by the University of Illinois at Chicago. We thank the NIH grant 1S10RR025105-01 for supporting the high-field NMR instruments used for structural characterization.

ACKNOWLEDGMENT

We thank Prof. Stephanie Cologna and K.P. Chandimal Pathmasiri for assistance with the collection and analysis of mass spectrometry data.

REFERENCES

(1) Periana, R. A.; Bhalla, G.; Tenn, W. J.; Young, K. J. H.; Liu, X. Y.; Mironov, O.; Jones, C.; Ziatdinov, V. R. Perspectives on Some Challenges and Approaches for Developing the next Generation of Selective, Low Temperature, Oxidation Catalysts for Alkane Hydroxylation Based on the CH Activation Reaction. *J. Mol. Catal. Chem.* **2004**, *220* (1), 7–25. https://doi.org/10.1016/j.molcata.2004.05.036.

(2) Tang, X.; Jia, X.; Huang, Z. Challenges and Opportunities for Alkane Functionalisation Using Molecular Catalysts. *Chem. Sci.* **2018**, *9* (2), 288–299. https://doi.org/10.1039/C7SC03610H.

(3) Goldberg, K. I.; Goldman, A. S. Large-Scale Selective Functionalization of Alkanes. *Acc. Chem. Res.* **2017**, *50* (3), 620–626. https://doi.org/10.1021/acs.accounts.6b00621.

(4) Schwarz, H. Chemistry with Methane: Concepts Rather than Recipes. *Angew. Chem. Int. Ed.* **2011**, *50* (43), 10096–10115. https://doi.org/10.1002/anie.201006424.

(5) Olah, G. A. Beyond Oil and Gas: The Methanol Economy. *Angew. Chem. Int. Ed.* **2005**, *44* (18), 2636–2639. https://doi.org/10.1002/anie.200462121.

(6) Chen, K.; Que, L. Stereospecific Alkane Hydroxylation by Non-Heme Iron Catalysts: Mechanistic Evidence for an $Fe^{V}O$ Active Species. *J. Am. Chem. Soc.* **2001**, *123* (26), 6327–6337. https://doi.org/10.1021/ja010310x.

(7) White, M. C.; Zhao, J. Aliphatic C–H Oxidations for Late-Stage Functionalization. *J. Am. Chem. Soc.* **2018**, *140* (43), 13988–14009. https://doi.org/10.1021/jacs.8b05195.

(8) Chen, M. S.; White, M. C. A Predictably Selective Aliphatic C H Oxidation Reaction for Complex Molecule Synthesis. *Science* **2007**, *318* (5851), 783–787. https://doi.org/10.1126/science.1148597.

(9) Olivo, G.; Farinelli, G.; Barbieri, A.; Lanzalunga, O.; Di Stefano, S.; Costas, M. Supramolecular Recognition Allows Remote, Site-Selective C–H Oxidation of Methylenic Sites in Linear Amines. *Angew. Chem.* **2017**, *129* (51), 16565–16569. https://doi.org/10.1002/ange.201709280.

(10) Schlichting, I. The Catalytic Pathway of Cytochrome P450cam at Atomic Resolution. *Science* **2000**, *287* (5458), 1615–1622. https://doi.org/10.1126/science.287.5458.1615.

(11) Ortiz de Montellano, P. R. Hydrocarbon Hydroxylation by Cytochrome P450 Enzymes. *Chem. Rev.* **2010**, *110* (2), 932–948. https://doi.org/10.1021/cr9002193.

(12) MacBeth, C. E.; Golombek, A. P.; Young, V. G.; Yang, C.; Kuczera, K.; Hendrich, M. P.; Borovik, A. S. O2 Activation by Nonheme Iron Complexes: A Monomeric Fe(III)-Oxo Complex Derived From O2. *Science* **2000**, *289* (5481), 938–941. https://doi.org/10.1126/science.289.5481.938.

(13) Shook, R. L.; Borovik, A. S. Role of the Secondary Coordination Sphere in Metal-Mediated Dioxygen Activation. *Inorg. Chem.* **2010**, *49* (8), 3646–3660. https://doi.org/10.1021/ic901550k.

(14) Breslow, R.; Zhang, X.; Huang, Y. Selective Catalytic Hydroxylation of a Steroid by an Artificial Cytochrome P-450 Enzyme. *J. Am. Chem. Soc.* **1997**, *119* (19), 4535–4536. https://doi.org/10.1021/ja9704951.

(15) Olivo, G.; Capocasa, G.; Lanzalunga, O.; Di Stefano, S.; Costas, M. Enzyme-like Substrate-Selectivity in C–H Oxidation Enabled by Recognition. *Chem. Commun.* **2019**, *55* (7), 917–920. https://doi.org/10.1039/C8CC09328H.

(16) Das, S. Molecular Recognition in the Selective Oxygenation of Saturated C-H Bonds by a Dimanganese Catalyst. *Science* **2006**, *312* (5782), 1941–1943. https://doi.org/10.1126/science.1127899.

(17) Vidal, D.; Costas, M.; Lledó, A. A Deep Cavitand Receptor Functionalized with Fe(II) and Mn(II) Aminopyridine Complexes for Bioinspired Oxidation Catalysis. *ACS Catal.* **2018**, *8* (4), 3667–3672. https://doi.org/10.1021/acscatal.7b04426.

(18) Groves, J. T.; Neumann, R. Enzymic Regioselectivity in the Hydroxylation of Cholesterol Catalyzed by a Membrane-Spanning Metalloporphyrin. *J. Org. Chem.* **1988**, *53* (16), 3891–3893. https://doi.org/10.1021/jo00251a054.

(19) Breslow, R. Biomimetic Chemistry and Artificial Enzymes: Catalysis by Design. *Acc. Chem. Res.* **1995**, *28* (3), 146–153. https://doi.org/10.1021/ar00051a008.

(20) Aravinda, S.; Shamala, N.; Balaram, P. Aib Residues in Peptaibiotics and Synthetic Sequences: Analysis of Nonhelical Conformations. *Chem. Biodivers.* **2008**, *5* (7), 1238–1262. https://doi.org/10.1002/cbdv.200890112.

(21) Karle, I. L. Controls Exerted by the Aib Residue: Helix Formation and Helix Reversal. *Pept. Sci.* **2001**, *60* (5), 351–365. https://doi.org/10.1002/1097-0282(2001)60:5<351::AID-BIP10174>3.0.CO;2-U.

(22) Karle, I. L.; Balaram, P. Structural Characteristics of .Alpha.-Helical Peptide Molecules Containing Aib Residues. *Biochemistry* **1990**, *29* (29), 6747–6756. https://doi.org/10.1021/bi00481a001.

(23) Banerjee, R.; Chattopadhyay, S.; Basu, G. Conformational Preferences of a Short Aib/Ala-Based Water-Soluble Peptide as a Function of Temperature: Aib/Ala-Based Peptide as a Function of Temperature. *Proteins Struct. Funct. Bioinforma.* **2009**, *76* (1), 184–200. https://doi.org/10.1002/prot.22337.

(24) Lombardi, A.; Nastri, F.; Pavone, V. Peptide-Based Heme–Protein Models. *Chem. Rev.* **2001**, *101* (10), 3165–3190. https://doi.org/10.1021/cr000055j.

(25) Yu, F.; Cangelosi, V. M.; Zastrow, M. L.; Tegoni, M.; Plegaria, J. S.; Tebo, A. G.; Mocny, C. S.; Ruckthong, L.; Qayyum, H.; Pecoraro, V. L. Protein Design: Toward Functional Metalloenzymes. *Chem. Rev.* **2014**, *114* (7), 3495–3578. https://doi.org/10.1021/cr400458x.

(26) Zastrow, M. L.; Peacock, A. F. A.; Stuckey, J. A.; Pecoraro, V. L. Hydrolytic Catalysis and Structural Stabilization in a Designed Metalloprotein. *Nat. Chem.* **2012**, *4* (2), 118–123. https://doi.org/10.1038/nchem.1201.

(27) Chino, M.; Maglio, O.; Nastri, F.; Pavone, V.; DeGrado, W. F.; Lombardi, A. Artificial Diiron Enzymes with a De Novo Designed Four-Helix Bundle Structure. *Eur. J. Inorg. Chem.* **2015**, *2015* (21), 3371–3390. https://doi.org/10.1002/ejic.201500470.

(28) Di Costanzo, L.; Wade, H.; Geremia, S.; Randaccio, L.; Pavone, V.; DeGrado, W. F.; Lombardi, A. Toward the de Novo Design of a Catalytically Active Helix Bundle: A Substrate-Accessible Carboxylate-Bridged Dinuclear Metal Center. *J. Am. Chem. Soc.* **2001**, *123* (51), 12749–12757. https://doi.org/10.1021/ja010506x.

(29) Cheng, R. P.; Fisher, S. L.; Imperiali, B. Metallopeptide Design: Tuning the Metal Cation Affinities with Unnatural Amino Acids and Peptide Secondary Structure. *J. Am. Chem. Soc.* **1996**, *118* (46), 11349–11356. https://doi.org/10.1021/ja9619723.

(30) Gibney, B. R.; Mulholland, S. E.; Rabanal, F.; Dutton, P. L. Ferredoxin and Ferredoxin–Heme Maquettes. *Proc. Natl. Acad. Sci.* **1996**, *93* (26), 15041–15046. https://doi.org/10.1073/pnas.93.26.15041.

(31) Sasaki, T.; Kaiser, E. T. Helichrome: Synthesis and Enzymic Activity of a Designed Hemeprotein. *J. Am. Chem. Soc.* **1989**, *111* (1), 380–381. https://doi.org/10.1021/ja00183a065.

(32) Sambasivan, R.; Ball, Z. T. Metallopeptides for Asymmetric Dirhodium Catalysis. *J. Am. Chem. Soc.* **2010**, *132* (27), 9289–9291. https://doi.org/10.1021/ja103747h.

(33) Coquière, D.; Bos, J.; Beld, J.; Roelfes, G. Enantioselective Artificial Metalloenzymes Based on a Bovine Pancreatic Polypeptide Scaffold. *Angew. Chem. Int. Ed.* **2009**, *48* (28), 5159–5162. https://doi.org/10.1002/anie.200901134.

(34) Vitale, R.; Lista, L.; Cerrone, C.; Caserta, G.; Chino, M.; Maglio, O.; Nastri, F.; Pavone, V.; Lombardi, A. An Artificial Heme-Enzyme with Enhanced Catalytic Activity: Evolution, Functional Screening and Structural Characterization. *Org. Biomol. Chem.* **2015**, *13* (17), 4859–4868. https://doi.org/10.1039/C5OB00257E.

(35) Lewis, J. C. Artificial Metalloenzymes and Metallopeptide Catalysts for Organic Synthesis. *ACS Catal.* **2013**, *3* (12), 2954–2975. https://doi.org/10.1021/cs400806a.

(36) Cussó, O.; Giuliano, M. W.; Ribas, X.; Miller, S. J.; Costas, M. A Bottom up Approach towards Artificial Oxygenases by Combining Iron Coordination Complexes and Peptides. *Chem. Sci.* **2017**, *8* (5), 3660–3667. https://doi.org/10.1039/C7SC00099E.

(37) Firpo, V.; Le, J. M.; Pavone, V.; Lombardi, A.; Bren, K. L. Hydrogen Evolution from Water Catalyzed by Cobalt-Mimochrome VI*a, a Synthetic Mini-Protein. *Chem. Sci.* **2018**, *9* (45), 8582–8589. https://doi.org/10.1039/C8SC01948G.

(38) Britovsek, G. J. P.; England, J.; White, A. J. P. Iron(Ii), Manganese(Ii) and Cobalt(Ii) Complexes Containing Tetradentate Biphenyl-Bridged Ligands and Their Application in Alkane Oxidation Catalysis. *Dalton Trans.* **2006**, No. 11, 1399. https://doi.org/10.1039/b513886h.

(39) Lister, F. G. A.; Le Bailly, B. A. F.; Webb, S. J.; Clayden, J. Ligand-Modulated Conformational Switching in a Fully Synthetic Membrane-Bound Receptor. *Nat. Chem.* **2017**, *9* (5), 420–425. https://doi.org/10.1038/nchem.2736.

(40) Eccles, N.; Le Bailly, B. A. F.; della Sala, F.; Vitórica-Yrezábal, I. J.; Clayden, J.; Webb, S. J. Remote Conformational Responses to Enantiomeric Excess in Carboxylate-Binding Dynamic Foldamers. *Chem. Commun.* **2019**, *55* (63), 9331–9334. https://doi.org/10.1039/C9CC03895G.

(41) Rittle, J.; Field, M. J.; Green, M. T.; Tezcan, F. A. An Efficient, Step-Economical Strategy for the Design of Functional Metalloproteins. *Nat. Chem.* **2019**, *11* (5), 434–441. https://doi.org/10.1038/s41557-019-0218-9.

(42) Tam, J. P.; Wu, C. R.; Liu, W.; Zhang, J. W. Disulfide Bond Formation in Peptides by Dimethyl Sulfoxide. Scope and Applications. *J. Am. Chem. Soc.* **1991**, *113* (17), 6657–6662. https://doi.org/10.1021/ja00017a044.

(43) Collins, J. M.; Porter, K. A.; Singh, S. K.; Vanier, G. S. High-Efficiency Solid Phase Peptide Synthesis (*HE* -SPPS). *Org. Lett.* **2014**, *16* (3), 940–943. https://doi.org/10.1021/ol4036825.

(44) Kelly, S. M.; Jess, T. J.; Price, N. C. How to Study Proteins by Circular Dichroism. *Biochim. Biophys. Acta BBA - Proteins Proteomics* **2005**, *1751* (2), 119–139. https://doi.org/10.1016/j.bbapap.2005.06.005.

(45) Greenfield, N. J. Using Circular Dichroism Spectra to Estimate Protein Secondary Structure. *Nat. Protoc.* **2006**, *1* (6), 2876–2890. https://doi.org/10.1038/nprot.2006.202.

(46) Vidal, D.; Costas, M.; Lledó, A. A Deep Cavitand Receptor Functionalized with Fe(II) and Mn(II) Aminopyridine Complexes for Bioinspired Oxidation Catalysis. *ACS Catal.* **2018**, *8* (4), 3667–3672. https://doi.org/10.1021/acscatal.7b04426.

(47) Tunstad, L. M.; Tucker, J. A.; Dalcanale, E.; Weiser, J.; Bryant, J. A.; Sherman, J. C.; Helgeson, R. C.; Knobler, C. B.; Cram, D. J. Host-Guest Complexation. 48. Octol Building Blocks for Cavitands and Carcerands. *J. Org. Chem.* **1989**, *54* (6), 1305–1312. https://doi.org/10.1021/jo00267a015.

(48) Hull, J. F.; Sauer, E. L. O.; Incarvito, C. D.; Faller, J. W.; Brudvig, G. W.; Crabtree, R. H. Manganese Catalysts with Molecular Recognition Functionality for Selective Alkene Epoxidation. *Inorg. Chem.* **2009**, *48* (2), 488–495. https://doi.org/10.1021/ic8013464.

(49) Iwasawa, T.; Wash, P.; Gibson, C.; Rebek, J. Reaction of an Introverted Carboxylic Acid with Carbodiimide. *Tetrahedron* **2007**, *63* (28), 6506–6511. https://doi.org/10.1016/j.tet.2007.03.075.

(50) Melton, L. D.; Slessor, K. N. Synthesis of Monosubstituted Cyclohexaamyloses. *Carbohydr. Res.* **1971**, *18* (1), 29–37. https://doi.org/10.1016/S0008-6215(00)80256-6.

(51) Armen, R.; Alonso, D. O. V.; Daggett, V. The Role of α-, 310-, and π-Helix in Helix→coil Transitions. *Protein Sci.* **2003**, *12* (6), 1145–1157. https://doi.org/10.1110/ps.0240103.

(52) Berger, A.; Loewenstein, A.; Meiboom, S. Nuclear Magnetic Resonance Study of the Protolysis and Ionization of N-Methylacetamide ^{1}. *J. Am. Chem. Soc.* **1959**, *81* (1), 62–67. https://doi.org/10.1021/ja01510a014.

(53) Oloo, W. N.; Banerjee, R.; Lipscomb, J. D.; Que, L. Equilibrating (L)Fe ^{III} –OOAc and (L)Fe ^{V} (O) Species in Hydrocarbon Oxidations by Bio-Inspired Nonheme Iron Catalysts Using H_2O_2 and AcOH. *J. Am. Chem. Soc.* **2017**, *139* (48), 17313–17326. https://doi.org/10.1021/jacs.7b06246.

(54) Oloo, W. N.; Que, L. Bioinspired Nonheme Iron Catalysts for C–H and C═C Bond Oxidation: Insights into the Nature of the Metal-Based Oxidants. *Acc. Chem. Res.* **2015**, *48* (9), 2612–2621. https://doi.org/10.1021/acs.accounts.5b00053.

(55) Fujita, M.; Que, L. In Situ Formation of Peracetic Acid in Iron-Catalyzed Epoxidations by Hydrogen Peroxide in the Presence of Acetic Acid. *Adv. Synth. Catal.* **2004**, *346* (2–3), 190–194. https://doi.org/10.1002/adsc.200303204.

(56) Mas-Balleste, R.; Que, L. Iron-Catalyzed Olefin Epoxidation in the Presence of Acetic Acid: Insights into the Nature of the Metal-Based Oxidant. *J. Am. Chem. Soc.* **2007**, *129* (51), 15964–15972. https://doi.org/10.1021/ja075115i.

(57) Williams, B. J.; Kmiec, K. L.; Russell, W. K.; Russell, D. H. Effect of Cysteic Acid Position on the Negative Ion Fragmentation of Proteolytic Derived Peptides. *J. Am. Soc. Mass Spectrom.* **2011**, *22* (1), 31–37. https://doi.org/10.1007/s13361-010-0009-4.

(58) Empting, M.; Avrutina, O.; Meusinger, R.; Fabritz, S.; Reinwarth, M.; Biesalski, M.; Voigt, S.; Buntkowsky, G.; Kolmar, H. "Triazole Bridge": Disulfide-Bond Replacement by Ruthenium-Catalyzed Formation of 1,5-Disubstituted 1,2,3-Triazoles. *Angew. Chem. Int. Ed.* **2011**, *50* (22), 5207–5211. https://doi.org/10.1002/anie.201008142.

(59) Knerr, P. J.; Tzekou, A.; Ricklin, D.; Qu, H.; Chen, H.; van der Donk, W. A.; Lambris, J. D. Synthesis and Activity of Thioether-Containing Analogues of the Complement Inhibitor Compstatin. *ACS Chem. Biol.* **2011**, *6* (7), 753–760. https://doi.org/10.1021/cb2000378.

(60) Akondi, K. B.; Muttenthaler, M.; Dutertre, S.; Kaas, Q.; Craik, D. J.; Lewis, R. J.; Alewood, P. F. Discovery, Synthesis, and Structure–Activity Relationships of Conotoxins. *Chem. Rev.* **2014**, *114* (11), 5815–5847. https://doi.org/10.1021/cr400401e.

TOC Graphic: